Hindawi
Journal of Nanomaterials
Volume 2022, Article ID 8739993, 17 pages
https://doi.org/10.1155/2022/8739993

Research Article

Sequential and/or Simultaneous Wet-Impregnation Impact on the Mesoporous Pt/Sn/Zn/γ-Al_2O_3 Catalysts for the Direct Ethane Dehydrogenation

Arshid M. Ali, Abdulrahim A. Zahrani, Muhammad A. Daous, Seetharamulu Podila, Majid Khalid Alshehri, Sami-ullah Rather, and Usman Saeed

Department of Chemical and Materials Engineering, Faculty of Engineering, King Abdulaziz University, Jeddah, Saudi Arabia

Correspondence should be addressed to Arshid M. Ali; arshid.mahmood.ali@gmail.com
and Sami-ullah Rather; rathersami@kau.edu.sa

Received 27 September 2021; Revised 6 January 2022; Accepted 28 January 2022; Published 23 February 2022

Academic Editor: Vincenzo Baglio

This study is aimed at investigating the impact of catalyst preparation's approach (either sequential and/or simultaneous wet impregnation) to a mesoporous series of Pt/A, Sn/A, PtSn/A, SnPt/A, (PtSn)/A, (PtSn)Zn/A, and (PtSnZn)/A catalysts for direct ethane dehydrogenation. The (PtSn)/A and (PtSnZn)/A had shown both higher initial specific activity (s^{-1}) and reaction rate constant K_d (h^{-1}) (13063.86 (s^{-1}) and 12489.69 (s^{-1}) and 0.09 (h^{-1}) and 0.06 (h^{-1})), respectively. The catalyst preparation approach had direct impact to the availability and dispersion of mesoporous particles of either active metal and/or promoter that influences either to hinder the C-C cleavage and/or to promote C-H bond cleavage in the dehydrogenation of ethane to ethene. The active metal component was present in the form of Pt, Pt^{+2}, Al^{+3}, Sn^{+4}, and Zn^{+2} states. The enhanced catalytic activity is attributed to the Pt_4Sn and PtZn formed phases in addition to highly dispersed mesoporous Pt particles. Based on the obtained results, the catalysts prepared by using simultaneous wet impregnation had shown higher catalytic activity and catalyst stability as to that of sequential wet impregnation.

1. Introduction

Ethylene is the main building blocks in process industry, and in the year 2021, its global production has surpassed 200 million tons per annum. The projected forecast of ethenes by the year 2025 is 290 million tons per annum. Olefins are more valuable compound than their predecessors, alkanes such as paraffin and ethane. Therefore, it is of industrial need to convert lower alkanes to respective alkenes. Multiple [1–46] have been reported for converting lower alkanes to their respective alkenes. Technologies like Catofins, fluidized bed reactor (FBD), UOP Oleflex, and STAR are seeking attention for propane dehydrogenation with trade-off reactor designs, catalyst type, regeneration mode, and % yield based on operating reaction temperature and pressure. However, aforementioned technologies are yet struggling to meet higher yield, catalyst stability, and life. Based on available literature, dehydrogenation was studied by using the following two approaches: oxidative and non-oxidative dehydrogenation [6, 12, 21, 25, 42, 47–55]. The low olefin selectivity and the formation of COX are major obstacles in ODH, whereas the NODH attained a better olefin yield. However, due to thermodynamic limitations, both technologies yet need to explore better options to enhance olefin yield with least undesired reaction products at reduced reaction temperature and pressure.

Usually, supported active metal/promoters were used in low alkane dehydrogenation. Based on initial literature assessment and known dehydrogenation literature for C1 to C4 alkanes, platinum [13, 20, 30, 31, 35, 51, 56–58] and chromium [37, 43, 49] are the commonly used catalyst. Each one of them has its own advantages and disadvantages. Pt has superior activation for C-H bond and low tendency towards C-C cleavage. It is highly stable and usually produces higher catalytic activity with low % loading in addition to environment friendly. However, sintering of Pt particles after frequent

Table 1: List of prepared catalyst by using either sequential and/or simultaneous wet impregnation.

Sr #	Catalyst composition	Brief to simultaneous/sequential	Notation
1	γ-Al_2O_3	-	A
2	1%Pt/γ-Al_2O_3	-	Pt/A
3	1%Sn/γ-Al_2O_3	-	Sn/A
4	1%Pt1%Sn/γ-Al_2O_3	*Sequential*: impregnation of Sn to Pt/γ-Al_2O_3 catalyst	PtSn/A
5	1%Sn1%Pt/γ-Al_2O_3	*Sequential*: impregnation of Pt to Sn/γ-Al_2O_3 catalyst	SnPt/A
6	1%Pt1%Sn/γ-Al_2O_3	Simultaneous impregnation of Pt and Sn to γ-Al_2O_3 support	(PtSn)/A
7	1%Pt1%Sn1%Zn/γ-Al_2O_3	*Sequential*: impregnation of Zn to (PtSn)/γ-Al_2O_3 catalyst	(PtSn)Zn/A
8	1%Pt1%Sn1%Zn/γ-Al_2O_3	Simultaneous impregnation of Pt, Sn, and Zn to γ-Al_2O_3 support	(PtSnZn)/A

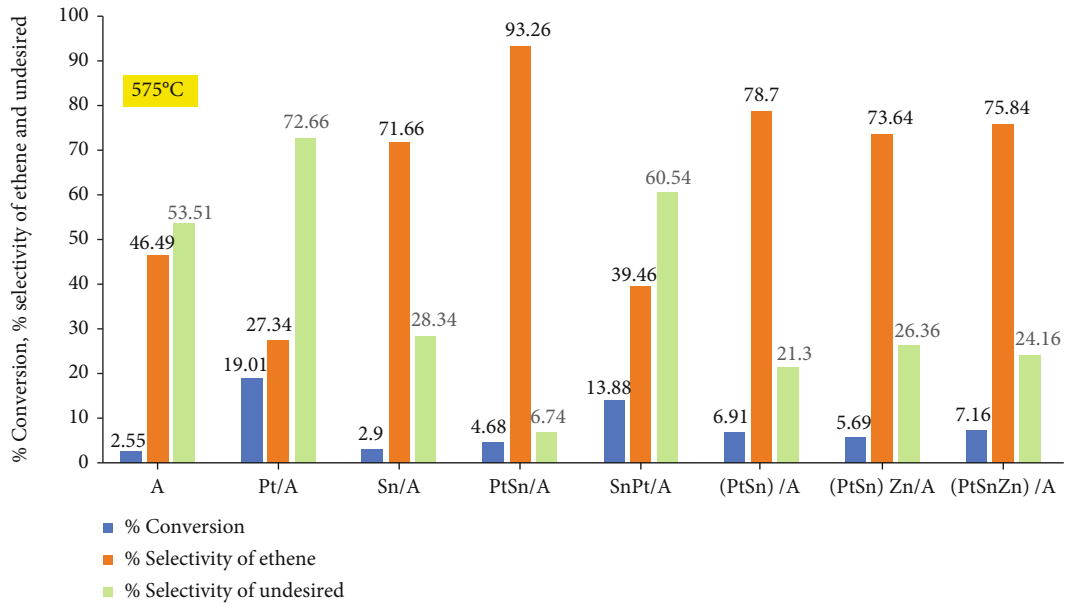

Figure 1: Catalytic activity comparisons of the support A and each of the freshly prepared Pt/A, Sn/A, PtSn/A, SnPt/A, (PtSn)/A, (PtSn)Zn/A, and (PtSnZn)/A catalysts at 575°C.

regeneration cycle can lead to decreased catalyst life, whereas the Cr metal has fair catalytic activity and selectivity dependent on Cr loading. However, Cr-based catalyst losses catalytic activity with each regeneration step due to decreased available surface area. In addition, it is environmentally toxic and has very little catalyst life in comparison to Pt metal. Therefore, many scientists and few commercial research and development organisation are yet inclined to use Pt as active metal for an efficient dehydrogenation catalyst for lower alkanes. In addition to active metal, the type and nature of the support of supported catalysts also played an important role. A crystalline framework arrangement with high surface area and uniform channel size is of acute importance. Based on available literature, the Pt-supported catalyst is preferred to meet current challenges of NODH.

Other than the selection of the best support, key aspect is to allow and/or control the formation of favorable phases of bi or multicomponent in the catalyst recipe. To address it, the catalyst preparation approach could play an important role to achieve the presence of more active phases. As of best knowledge of the authors, a very little scientific information on the comparison of the catalyst preparation approach such as sequential and/or simultaneous wet impregnation is available especially Pt-supported catalyst for NODH. Therefore, this study is aimed at preparing and comparing the catalytic activities of a methodologically prepared series of the catalysts (see Table 1) using either sequential and/or simultaneous wet impregnation. This approached has never been reported for lower alkane direct dehydrogenation. Such study shall shed an insight to the active metal dispersion and impact of preparation approach to form active phase between mono and/or binary active metal components.

2. Materials and Methods

The used chloride salts of platinum, tin, magnesium, calcium, and zinc were procured from Sigma-Aldrich. The list of used chemicals was Platinum(II) chloride (≥99.9% trace metals basis), Tin(II) chloride reagent grade (98%), Zinc chloride (99.999% trace metals basis), and deionized water. The catalyst support, γ-Al_2O_3 (SS-200), was obtained from BASF chemicals.

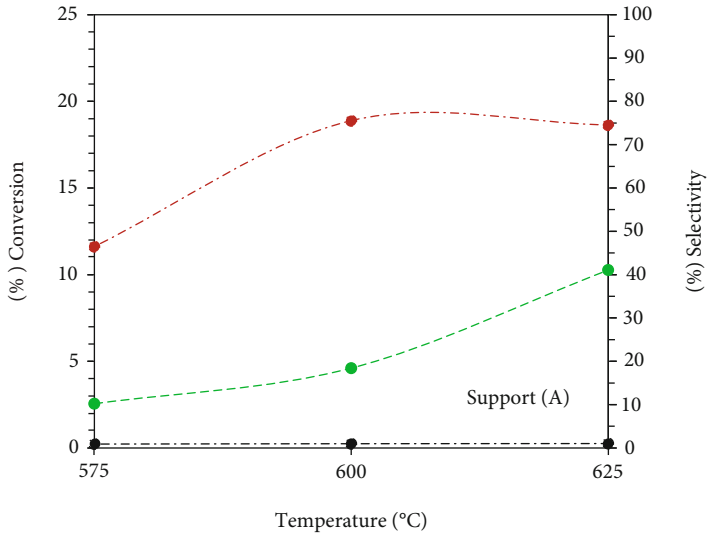

(a)

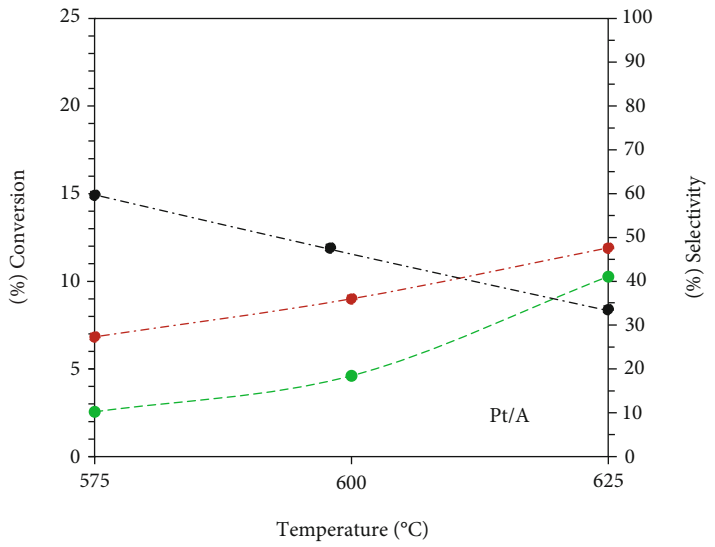

(b)

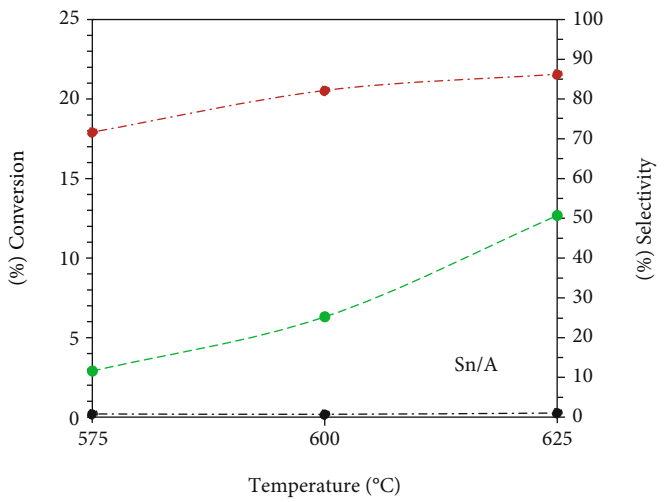

(c)

Figure 2: Continued.

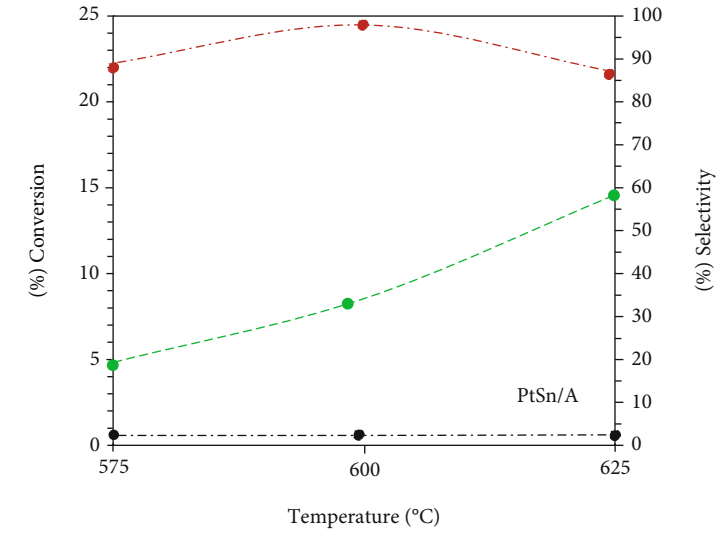

(d)

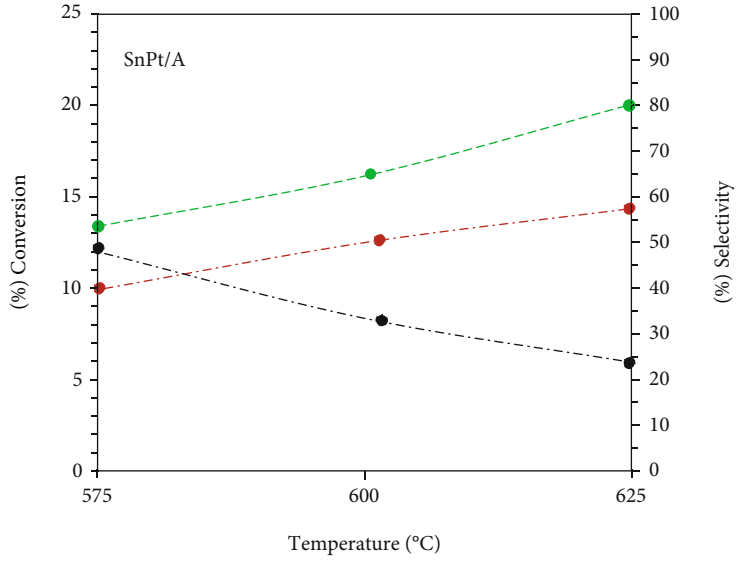

(e)

Figure 2: Continued.

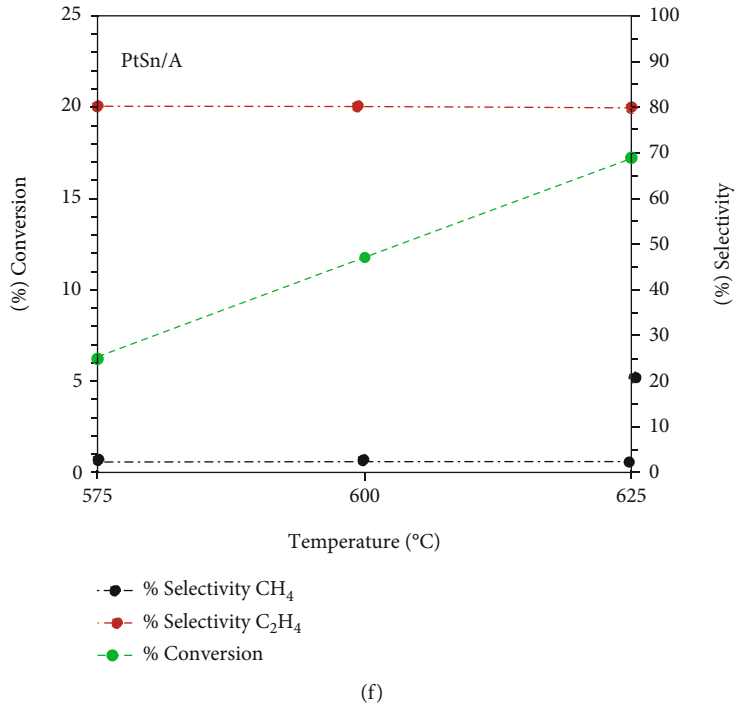

Figure 2: Effect of reaction temperature to the catalytic activity of the support A, Pt/A, Sn/A, PtSn/A, SnPt/A, and (PtSn)/A catalysts.

2.1. Catalyst Preparation. The catalyst support γ-Al_2O_3 pallets were crushed to sieve size of 300–600 mesh size by using the grinder (ERWEKA AR 402, TG2000) and were calcined at 650°C for 6 hours under static air. All the catalysts were prepared by using wet impregnation at 85°C for 5 hours. A precise amount of well-dried catalyst support and 1% active metal precursor stock solution were added to rotary evaporator to prepare a series of the catalyst by using sequential and/or simultaneous approach (see Table 1). The impregnated sludge was dried in a digitally controlled vacuum dryer at 110°C for 4 hours. The dried impregnated sludge was multiply rinsed with deionized water to remove any chloride residues. Finally, it was calcined for a time of 6 hours at 650°C under flowing air (100 ml/min) using a tube furnace. The calcined catalyst samples were converted into small tablets by using tablet press machine. At the end, the catalyst tablet was crushed to particle size of 125-250 μm.

2.2. Catalytic Activity. The catalytic activity of freshly prepared catalysts was tested in a PID Microactivity reactor (PID ENG & TECH) coupled with online gas chromatography (GC; 7890B-Agilent) containing both flame ionization and thermal conductivity detectors (FID and TCD). Both safety and absence of any leaks in PID Microactivity reactors were tested by using an inert gas nitrogen with a flow rate of 8.8 ml/min for 1 hour at 600°C. Before the catalytic run, the catalyst was reduced at 600°C. After the catalyst reduction, N_2 was used to purge any traces of unwanted gas/media. 0.5 g of reduced catalyst as loaded to the reactor and the catalytic activity of each catalyst was tested at three different temperatures 575°C, 600°C, and 625°C under flow rate of in the ratio of $N_2 : H_2 : C_2H_6 = 3 : 1 : 1$. The catalytic activity at each temperature is monitored and recorded for 2 hrs. The total reaction time was 6.7 hours. Throughout the reaction, the extent of conversion of ethane to ethylene and/or other unwanted products was measured by using GC.

2.3. Catalyst Characterization. Micrometer NOVA 2200e analyzer was used to measure the BET surface area and pore distribution by using N_2-physiosorption method. X-ray diffraction (XRD) was used to study the crystalline phase of both unused and used catalyst at 25°C with 2θ range of 20–120°C by using Equinox 1000 equipped with Co-kα radiation. A SPECS GmbH X-ray photoelectron spectroscopy was used to identify the oxidation states of the active metal by using dual nonmonochromatic X-ray source Al-Kα under 13.5 kV, 150 Watts of X-ray power. H_2-temperature programmed reduction was used to analyze the redox behavior of 0.6 g of spent catalyst from room temperature to 875°C with 15 ml/min flow of 5% H_2/N_2 gas. Quantachrome pulsar automatic chemisorption analyzer equipped with ThermoStar TM GSD 320 quad core mass spectrometer was used to study the NH_3-temperature programmed desorption for acid-base behavior and dispersion of active metal.

3. Results and Discussions

3.1. Catalytic Activity. PID Microactivity reactor was used to study the catalytic activity of the support A and each of the freshly prepared Pt/A, Sn/A, PtSn/A, SnPt/A, (PtSn)/A, (PtSn)Zn/A, and (PtSnZn)/A catalysts. The % conversion, % selectivity of ethene, and undesired reaction products obtained at 575°C are shown in Figure 1. For the reported value of catalytic activity, selectivity is the average of the values obtained during 2 hrs reaction with standard deviation of 0.01%.

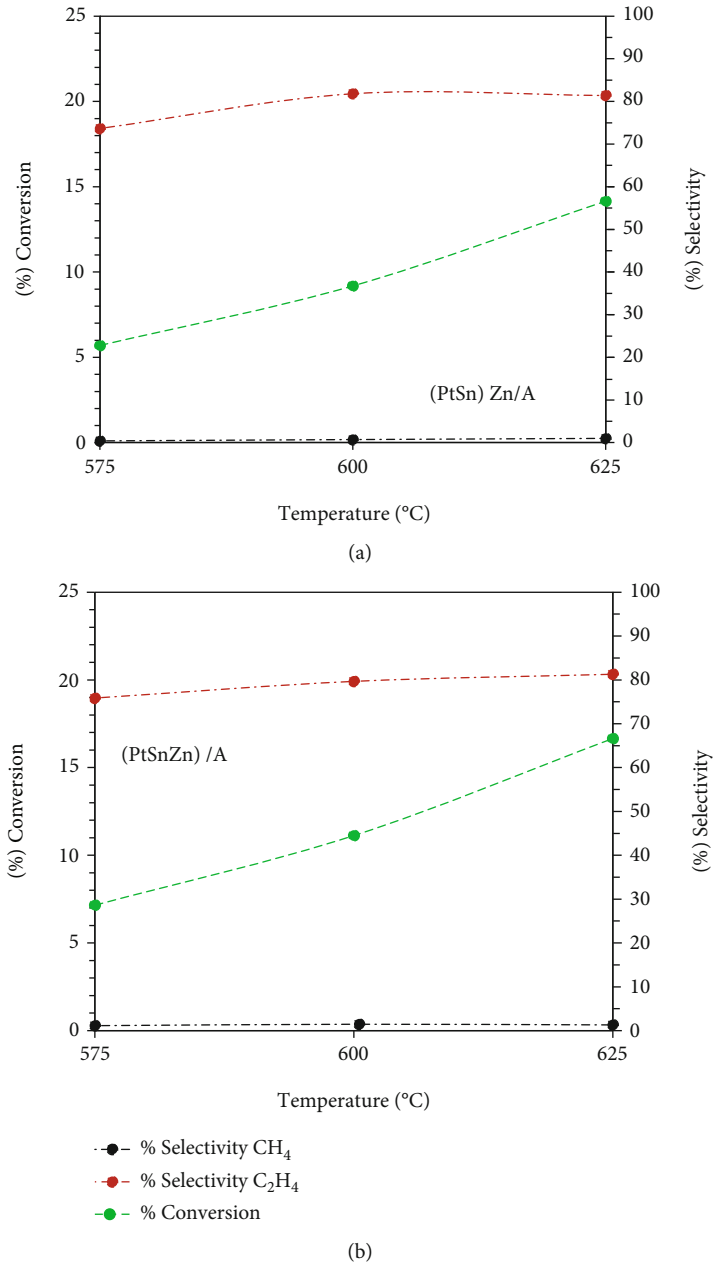

Figure 3: Effect of reaction temperature to the catalytic activity of the (PtSn)Zn/A and (PtSnZn)/A catalysts.

In the case of the catalyst support A, the % conversion of ethane, % selectivity of ethene, and % selectivity of the undesired reaction product were 2.55%, 46.49%, and 53.51%, respectively. Overall, the % selectivity of undesired reaction product is slightly higher as to that of % selectivity of desired product (ethene) with very little % conversion of ethane to ethene.

The Pt/A catalyst had shown 19.01% conversion, 27.34% ethene selectivity, and 72.66% selectivity of undesired reaction product. Overall, the Pt/A catalyst was more active as to that of the support A. However, it has shown very high % selectivity of undesired reaction products due to the Pt attack on C-C bond [59]. This led to higher cracking of ethane to methane and coke formation.

The Sn/A catalysts had shown 2.9% conversion, 71.66% ethene selectivity, and 28.34% selectivity of undesired reaction product. Overall, the Sn/A catalyst had shown lower % conversion in comparison to Pt/A catalyst. However, the Sn/A catalyst had shown reduced formation of undesired reaction products. This is because of the least ability of Sn in the catalyst composition to break C-C bonds and/or cracking [31]. In addition, the Sn has significantly assisted to reduce the acidic nature of the support [60].

The PtSn/A had shown 4.68% conversion of ethane with ethene % selectivity of 93.26% and 6.74% of undesired product selectivity. The PtSn/A catalyst had shown increased % conversion in comparison to the support and Sn/A catalyst. Also, the PtSn/A catalyst has shown the highest % selectivity

Table 2: A comparison of % conversion, % selectivity, and % yield of desired reaction product (ethene) at 575°C, 600°C, and 625°C.

Catalyst	% conversion Temperature (°C)			% selectivity Temperature (°C)			% yield Temperature (°C)		
	575	600	625	575	600	625	575	600	625
A	2.55	4.61	10.27	46.49	75.53	74.52	1.19	3.48	7.65
Pt/A	19.01	22.63	24.96	27.34	36.01	47.63	5.20	8.15	11.89
Sn/A	2.9	6.31	12.68	71.66	82.14	86.24	2.08	5.18	10.94
PtSn/A	4.68	7.73	12.69	93.26	98.5	92.12	4.36	7.61	11.69
SnPt/A	13.88	17.07	21.61	39.46	51.41	60.05	5.48	8.78	12.98
(PtSn)/A	6.91	11.78	16.63	78.7	78.60	78.26	5.44	9.26	13.01
(PtSn)Zn/A	5.69	9.18	14.15	73.64	81.81	81.39	4.19	7.51	11.52
(PtSnZn)/A	7.16	11.13	16.66	75.84	79.67	81.31	5.43	8.87	13.55

Table 3: Comparison of % metal, Pt/Sn and Pt/Zn ratio, % conversion, % selectivity, % yield, initial specific activity (s^{-1}), and reaction rate constant K_d (h^{-1}) for the reaction carried at 600°C.

Catalyst	Pt (% wt)	Sn (% wt)	Zn (% wt)	Pt/Sn	Pt/Zn	Conv. (%)	Sel. (%)	Yield (%)	Initial specific activity (s^{-1})	Reaction rate constant K_d (h^{-1})
(PtSn)/A	0.54	1.68	-	0.32	-	11.78	78.60	9.26	13063.86	0.09
(PtSnZn)/A	0.48	1.78	0.81	0.27	0.59	9.04	79.67	8.87	12489.69	0.06

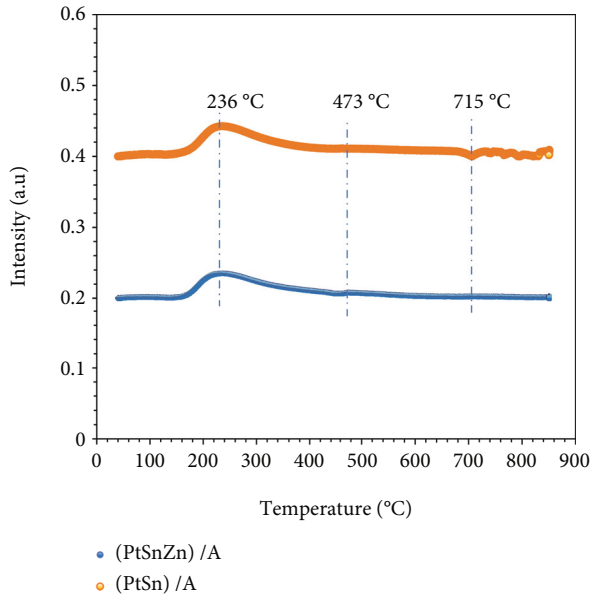

Figure 4: TPR analysis comparison between (PtSn)/A and (PtSnZn)/A catalyst.

of ethene in addition to least % selectivity of undesired reaction products. However, the % conversion of PtSn/A is lower than that of the Pt/A. This is because of the presence of Pt with Sn had reduced affinity to C-C bond—clear from the least % selectivity of undesired reaction product CH_4 (which can be only formed from the C-C bond cleavage in ethane molecule) [31, 60]. Overall, the PtSn/A has the highest % selectivity of ethene with least % selectivity of undesired reaction products.

The SnPt/A had shown 13.88% conversion of ethane to ethene with % selectivity of 39.46% and 60.54% of undesired product selectivity. In comparison, the SnPt/A catalyst had shown higher % conversion of ethane and % selectivity of undesired reaction products as to that of PtSn/A catalyst. This is because of highly dispersed mesoporous Pt particles at the outer surface of unhomogenized catalyst due to the sequential wet impregnation of Pt to Sn/A catalyst to obtain SnPt/A catalyst. The availability of highly dispersed mesoporous Pt in the unhomogenized catalyst led to the enhanced % conversion due to C-C cleavage rather due to C-H cleavage, mandatory for dehydrogenation of ethane [9, 34, 35, 37, 58, 59].

The (PtSn)/A catalyst exhibited 6.91% conversion of ethane, with ethene % selectivity of 78.7% and 21.3% of undesired product selectivity. The % of undesired reaction products, in the case of (PtSn)/A catalyst, was less than SnPt/A catalyst and higher as to that of PtSn/A catalyst. The (PtSn)/A, prepared by simultaneous wet impregnation of both Pt and Sn on the support A, has generated a better alloy between Pt and Sn due to which the individual impact of either Pt and/or Sn was reduced [33, 56]. That is why, the % conversion of (PtSn)/A is less as to that of either PtSn/A or SnPt/A due to trade of between cracking/C-C bond cleavage and the dehydrogenation.

The (PtSn)Zn/A catalyst exhibited 5.69% conversion of ethane, with ethene % selectivity of 73.64% and 26.36% of undesired product selectivity. These results showed that sequential addition of Zn to (PtSn)/A catalyst had not impacted much to the acidity of the catalyst support A due to which the (PtSn)Zn/A had shown lower % conversion as to that of (PtSn)/A catalyst. In parallel, the addition of the Zn to (PtSn)/A catalyst also led to the decreased C-C cleavage/cracking with enhanced dehydrogenation extent [37].

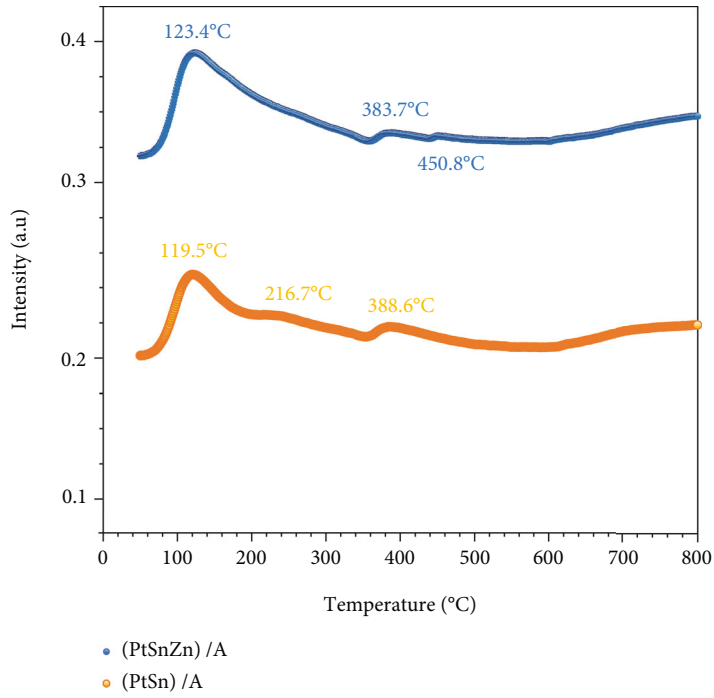

Figure 5: NH_3-TPD study comparison of (PtSn)/A and (PtSnZn)/A catalyst.

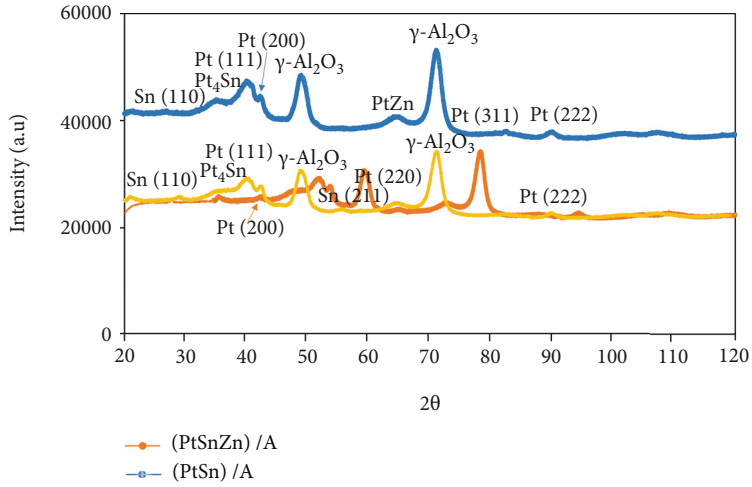

Figure 6: Comparison of XRD analysis of (PtSn)/A and (PtSnZn)/A catalysts.

Due to the favorable impact of Zn to (PtSn)/A catalyst, it was thought to prepare a (PtSnZn)/A catalyst by using the simultaneous impregnation of Pt, Sn, and Zn to the catalyst support. The (PtSnZn)/A catalyst exhibited 7.16% conversion of ethane, with ethene % selectivity of 75.84% and 24.16% of undesired product selectivity. The overall catalytic activity (in terms of % conversion, % selectivity of ethene, and undesired reaction products) of the (PtSnZn)/A catalyst is higher as to that of the (PtSn)Zn/A catalyst. This is clearly due to enhanced beneficial impacts of the simultaneous impregnation of Zn with Pt and Sn to the catalyst support which led to much better homogenized catalyst with better Pt-Sn/Sn-Zn/Pt-Zn alloy formation [31, 37, 60]. In addition, this catalyst preparation approach [2] led to significant decrease in C-C cleavage/cracking with higher dehydrogenation extent.

In general, the catalytic activity in terms of % conversion, % selectivity of ethene, and undesired reaction products is different either due to catalyst composition and/or catalyst preparation approach (sequential and/or simultaneous) within the single catalyst preparation method (wet impregnation).

3.2. Effect of Reaction Temperature. The effect of reaction temperature plays a significant role either to overall catalytic activity and/or stability of the catalyst. Therefore, the catalytic activity (in terms of % conversion, % selectivity of ethene, and undesired reaction product (ethane)) of all the

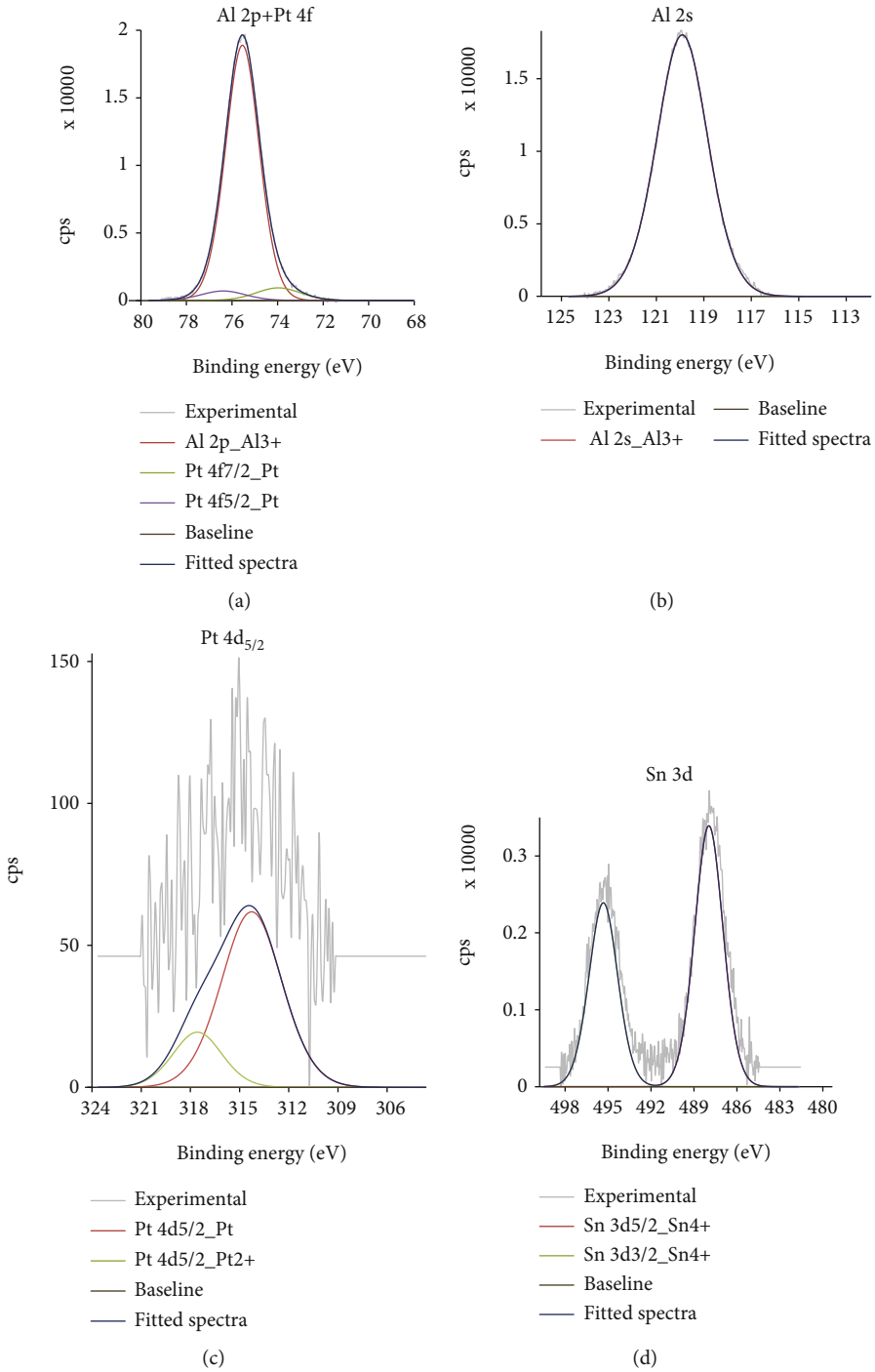

Figure 7: Continued.

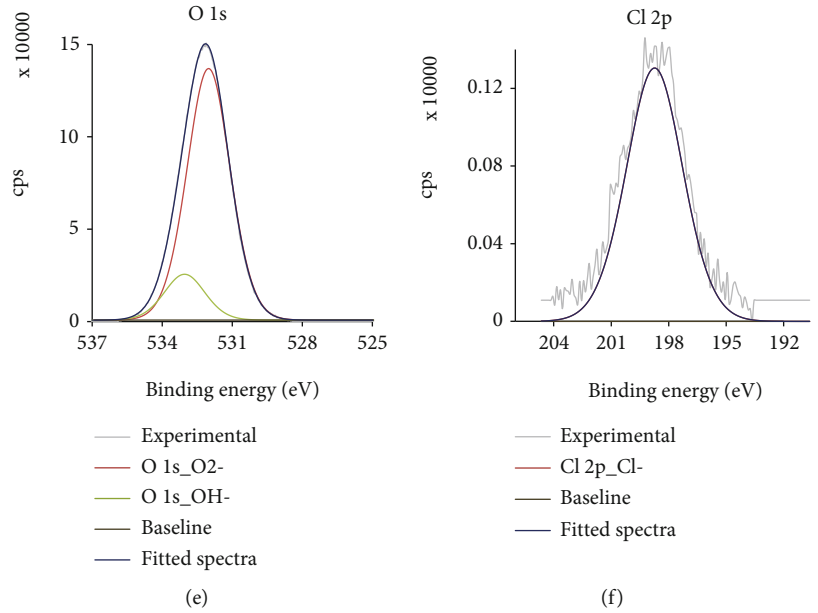

Figure 7: XPS analysis of (PtSn)/A. (a) The deconvoluted spectra of Al 2p+Pt4f. (b) The deconvoluted spectra of Al 2s. (c) The deconvoluted spectra of Pt 4d. (d) The deconvoluted spectra of Sn 3d. (e) The deconvoluted spectra of O 1s. (f) The deconvoluted spectra of Cl 2p.

catalysts was studied at three different reaction temperatures 575°C, 600°C, and 625°C. The effect of each reaction temperature is shown in Figures 2 and 3.

In general, % conversion increased with the increase in temperature for all the catalysts. However, the % selectivity of desired and undesired reaction product varies with the catalyst composition. For instance, the % selectivity of undesired reaction product (methane) at each studied reaction temperature (575°C, 600°C, and 625°C) was nearly remained constant for the support A and Sn/A, PtSn/A, (PtSn)/A, (PtSn)Zn/A, and (PtSnZn)/A catalysts (see Figures 2(a), 2(c), 2(d), 2(f), 3(a), and 3(b)). However, in the case of the Pt/A and SnPt/A catalysts, the % selectivity of methane (undesired reaction product) gradually decreased with the increase in reaction temperature (see Figures 2(b), 2(e), and 3(a)). This could be due to the freely available Pt mesoporous particles because it is well established that Pt has higher tendency to C-C bond cleavage [9, 34, 35, 37, 58, 59]. In other words, it is the least formation of potential active alloy phase(s) between Pt and Sn in the case of SnPt/A catalyst. Therefore, the catalyst preparation approach either sequential and/or simultaneous wet impregnation has direct influence to hinder the C-C and/or C-H bond cleavage in dehydrogenation.

In terms of % selectivity of the desired reaction product (ethane), it increased with the increase in reaction temperature for all the studied catalysts except the PtSn/A and (PtSn)/A catalysts. In the case of PtSn/A, the % selectivity of ethene first increases with the increase in the reaction temperature from 575°C to 600°C and then it decreased with the further reaction temperature increase from 600°C to 625°C (see Figure 2(d)), whereas in the case of the (PtSn)/A catalyst, the % selectivity of ethene remained almost constant with the increase in reaction temperature from 575°C to 625°C (see Figure 2(f)). In all other studied Pt/A, Sn/A, SnPt/A, (PtSn)Zn/A, and (PtSnZn)/A catalysts, the % selectivity of ethene increased with the increase in reaction temperature (see Figures 2(b), 2(c), 2(e), 3(a), and 3(b)). However, the extent of the increased % selectivity of ethane is different in each catalyst composition.

An overall comparison of % conversion, % selectivity, and % yield of desired reaction product (ethene) at 575°C, 600°C, and 625°C temperature is shown in Table 2. Among all the studied catalysts, the (PtSn)/A and (PtSnZn)/A showed maximum % yield of desired reaction product (ethene) at 575°C, 600°C, and 625°C, respectively. Both catalysts were prepared by using simultaneous wet impregnation.

Based on abovementioned findings, the initial specific activity (s^{-1}) and reaction rate constant K_d (h^{-1}) of the best (PtSn)/A and (PtSnZn)/A were calculated by using the following:

$$\text{Initial specific activity } \left(s^{-1}\right) = \frac{[\text{moles of the product/moles of Pt}]}{\text{time}},$$
$$\text{Reaction rate constant } K_d \left(h^{-1}\right) = \frac{[\ln(1 - x_{\text{end}})/x_{\text{end}}) - \ln(1 - x_{\text{start}})/x_{\text{start}})]}{\text{time}}, \quad (1)$$

where x_{end} and x_{start} are the conversion at the start and end of the reaction.

The summary of the results is shown in Table 3. In general, the catalyst preparation approach, either sequential and/or simultaneous wet impregnation, has direct link to the enhanced % selectivity and/or % yield of desired reaction product.

3.3. TPR Analysis. The TPR analysis is very useful to study the interaction of active metal with support and/or promoter. Based on the highest catalytic activity, in terms of

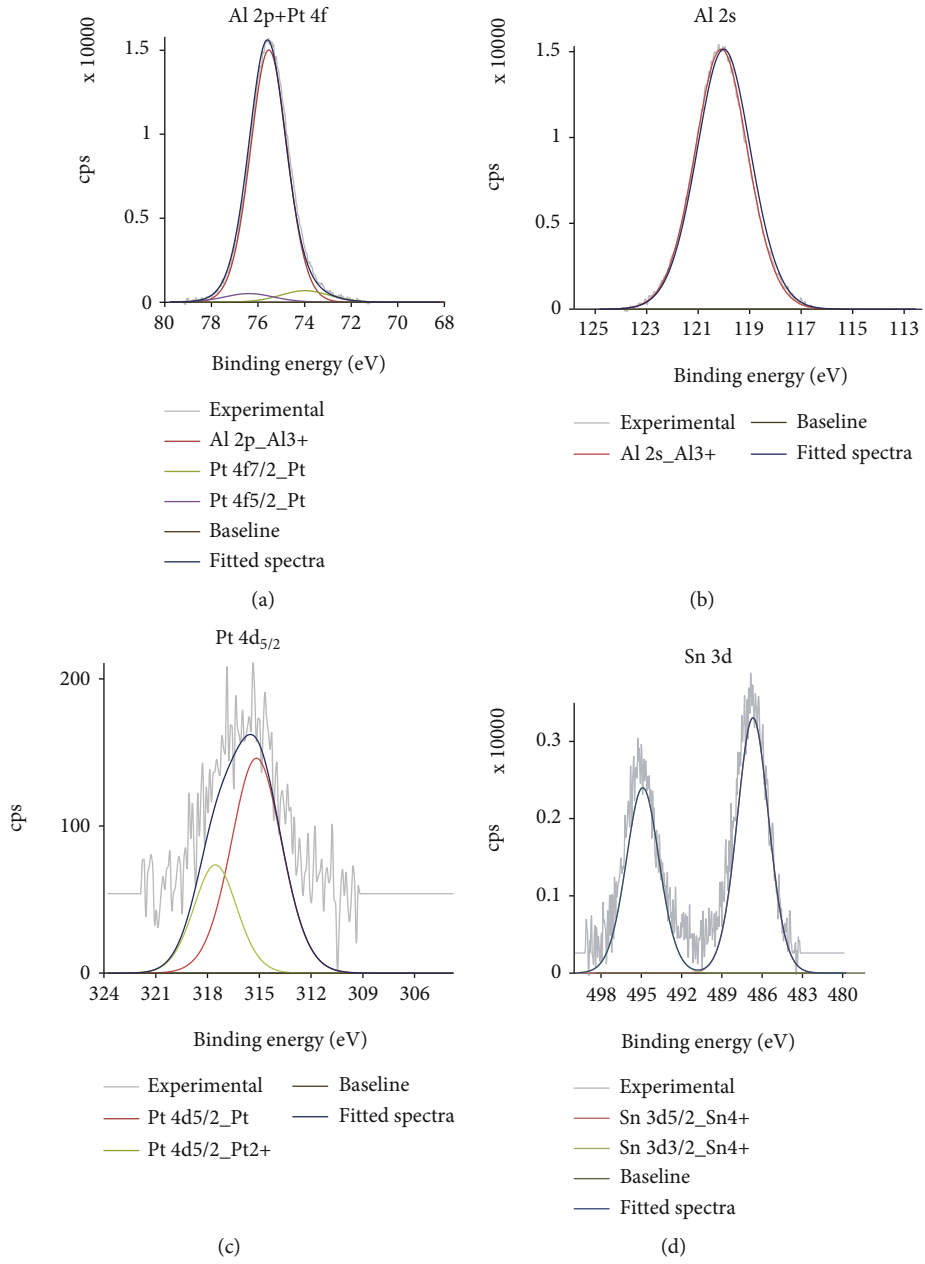

Figure 8: Continued.

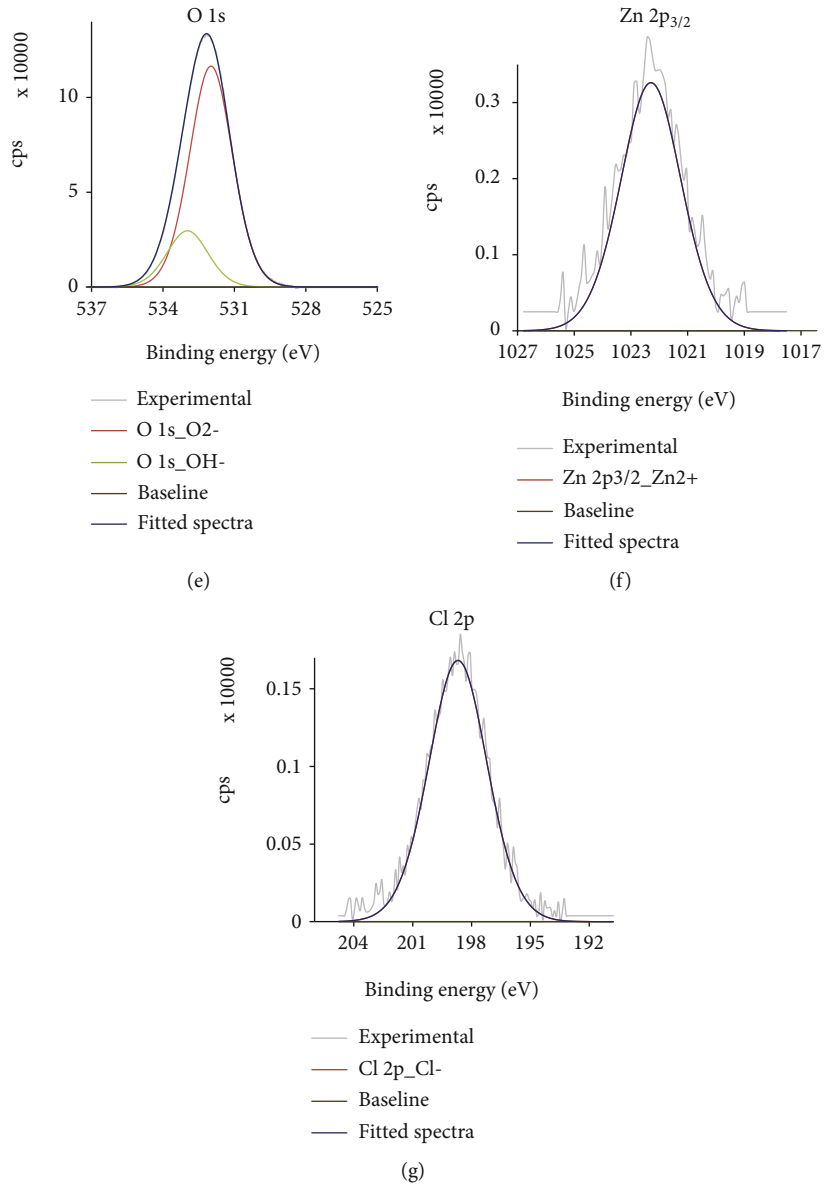

Figure 8: XPS analysis of (PtSnZn)/A. (a) The deconvoluted spectra of Al 2p+Pt4f. (b) The deconvoluted spectra of Al 2s. (c) The deconvoluted spectra of Pt 4d. (d) The deconvoluted spectra of Sn 3d. (e) The deconvoluted spectra of O 1s. (f) The deconvoluted spectra of Zn 2p. (g) The deconvoluted spectra of Cl 2p.

initial specific activity and reaction rate constant, the best (PtSn)/A and (PtSnZn)/A catalysts were analyzed by using TPR technique. The obtained results are shown in Figure 4. The (PtSn)/A catalyst exhibited comparatively intense and broader Pt peak at 236°C as to that of (PtSnZn)A catalyst at the same temperature. This peak belonged to Pt [61]. The slightly higher intensity of Pt peak, in (PtSn)/A catalyst, showed that it required more H_2 consumption to reduce Pt-O surface as to that of (PtSnZn)/A. This showed that dispersion of Pt mesoporous particles in (PtSn)/A catalyst is higher in comparison to (PtSnZn)/A catalyst. Due to better dispersion of Pt mesoporous particles, the (PtSn)/A catalyst had higher initial specific activity (13063.86 s^{-1}) and reaction rate constant K_d (h^{-1}) as to that of (PtSnZn)/A catalyst which had less initial specific activity and reaction constant (12489.69 s^{-1} and K_d (h^{-1}) of 0.06, respectively). In addition, the (PtSnZn)/A exhibited a minor peak at 473°C. This peak belonged to Zn [62]. The intensity of this peak showed very little dispersion of Zn mesoporous particle, and the presence of Zn with active metal Pt did not contribute much to enhance the overall catalytic activity of (PtSnZn)/A in terms of both initial specific activity and reaction rate constant.

3.4. NH_3-TPD Study. The catalytic activity of a supported catalyst depends on both catalyst preparation method and the surface acidity of the catalyst support (the acid-base behavior) which has direct impact to the dispersion of the active metal and/or promoter. To access such impact to the catalytic activity, both (PtSn)/A and (PtSnZn)/A catalysts were

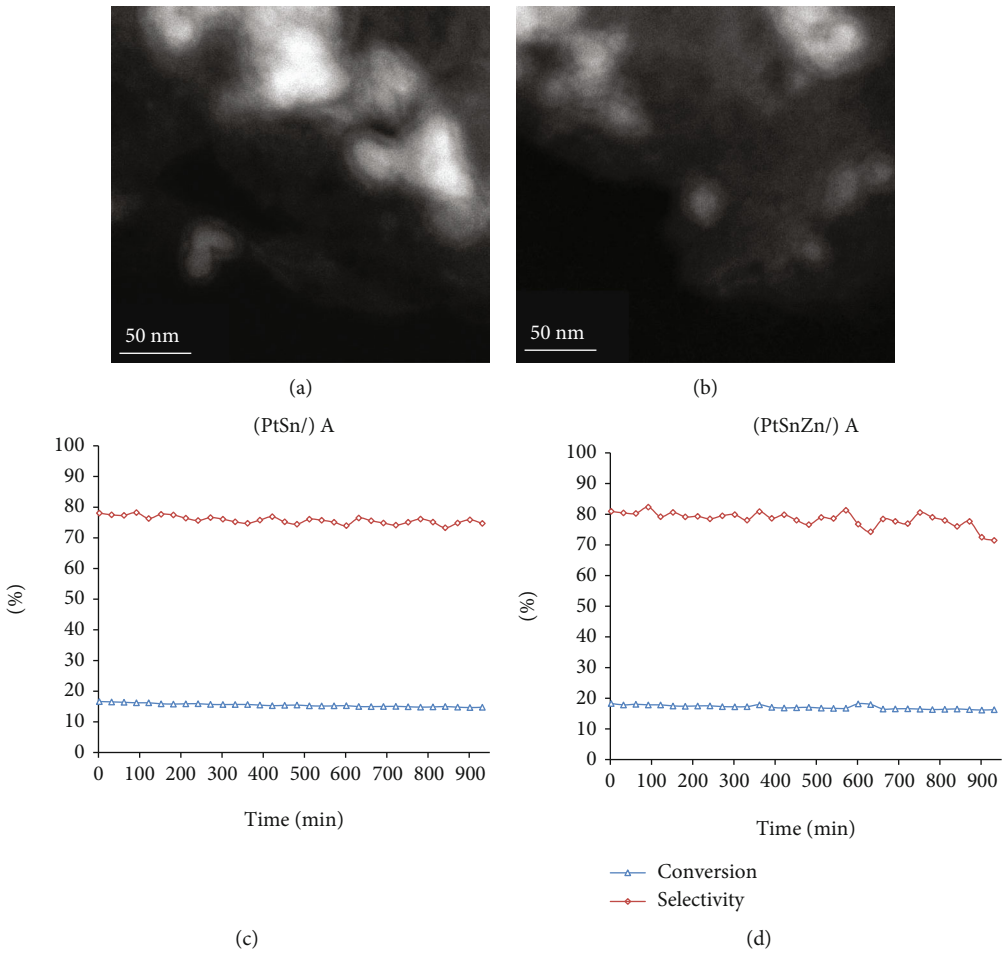

Figure 9: Comparison of TEM analysis and catalyst stability tests.

characterized by using NH_3-TPD technique. The obtained result is shown in Figure 5. Both (PtSn)/A and (PtSnZn)A exhibited different TPD curves. In the case of (PtSn)/A, the peak intensities are slightly less as to that of the peaks in (PtSnZn)/A catalyst. The low TPD peak intensity in (PtSn)/A corresponds to ammonia desorption from comparatively bit strong acidic sites. The slightly high intensity peaks of (PtSnZn)/A correspond to comparatively weak acidic sites. The extent of either weak and/or strong acid sites [63, 64] reflected to the unequal dispersion of the active metal Pt in each catalyst. Based on the results, the dispersion of Pt in (PtSn)/A was better as to that in (PtSnZn)/A catalyst. This leads to enhanced catalytic activity of (PtSn)/A both in terms of initial specific activity and reaction rate constant. However, the simultaneous addition of Zn, Sn, and Pt to the support leads to an overall decreased formation of undesired reaction products. Therefore, the presence of Zn in the catalyst's recipe increased the catalyst stability by suppressing the formation of undesired reaction products. Though, the overall catalytic activity of (PtSnZn)A is less as to that of (PtSn)/A. This could be attributed to active oxidation state(s) of metal, Pt/Sn, and/or Pt/Zn ratio, in addition to the formed Pt_xSn_y, Pt_xZn_y, and $Pt_xSn_yZn_z$ phases.

3.5. XRD Analysis. To investigate potential formation of Pt-Sn, Pt-Zn, and Pt-Sn-Zn phases in addition to the crystal orientation, both (PtSn)/A and (PtSnZn)/A catalysts were analyzed by using XRD analysis and results are shown in Figure 6.

The diffraction patterns of the (PtSnZn)/A catalyst exhibited Sn(110), Pt_4Sn, Pt(111), Pt(200), PtZn, Pt(311), and Pt(222) peaks in addition to the support γ-Al_2O_3 peaks [65, 66]. Among all the peaks attributed to the Pt, the Pt(111), Pt(311), and Pt(222) were the prominent as to that of Pt(200). A very less intense trace of Sn(110) and Pt_4Sn was also present in addition to PtZn peak in the (PtSnZn)/A catalyst. The (PtSn)/A had Sn(110), Pt_4Sn, Pt(111), Pt(200), Sn(211), Pt(220), and Pt(222) peaks in addition to γ-Al_2O_3 peaks. Among all the Pt peak, the Pt(111) and Pt(222) were the prominent in comparison to Pt(200) and Pt(220) peaks. Among Sn peaks, the Sn(110) was the prominent as to that of Sn(211) peak. In comparison, the Pt(220) and Pt (311) peaks were not found in both (PtSn)/A and (PtSnZn)A catalysts. The Pt(220) was identified in (PtSn)/A catalyst only, and the Pt(311) peak was present in the (PtSnZn)/A catalyst only. In addition, the (PtSnZn)/A exhibited a weak PtZn peak.

In brief, the different catalytic activity of (PtSn)/A and (PtSnZn)/A is attributed to the Pt_4Sn and PtZn phases in addition highly dispersed mesoporous Pt particles. Based on higher catalytic activity of (PtSn)/A catalyst, the presence

of Pt_4Sn phase is more beneficial as to that of PtZn phase. The formation of Pt_4Sn phase is attributed to the natural tendency of Pt towards Sn. Usually, the higher Pt/Sn ratio led to increased reaction rate.

3.6. XPS Analysis. To assess the metal ration and possible oxidation state of each active metal and surface chemical composition, both (PtSn)/A and (PtSnZn)/A catalysts were analyzed by using XPS. The results are shown in Figures 7 and 8.

The complete survey spectrum of (PtSn)/A catalyst exhibited Al 2p (73.64 eV), Al 2s (119.09 eV), Pt $4f_{5/2}$ (75.24 eV), Pt $4f_{7/2}$ (71.74 eV), Pt $4d_{5/2}$ (314.03 eV), Pt $4d_{5/2}$ (317.53 eV), Sn $3d_{5/2}$ (486.84 eV), and Sn $3d_{3/2}$ (494.99 eV) in addition to the O 1s and Cl 2p peaks. The deconvoluted Al 2p (73.64 eV) and Al 2s (119.09 eV) peaks of Al showed the presence of Al^{+3}, whereas the deconvoluted Pt $4d_{5/2}$ (314.03 eV) and Pt $4d_{5/2}$ (317.53 eV) peaks of Pt indicated the presence of Pt and Pt^{+2}, respectively. Finally, the Sn was present in the form of Sn^{+4} indicated by the deconvoluted Sn $3d_{5/2}$ (486.84 eV) and Sn $3d_{3/2}$ (317.53 eV) peaks of Sn. In summary, the active metal component of the (PtSn)/A catalyst was present in the form of Pt, Pt^{+2}, Al^{+3}, and Sn^{+4} ions. In addition, the Pt mesoporous particles were well dispersed within the support (see Figure 7(a); deconvolution exhibited the presence of both Al 2p and Pt 4f).

The (PtSnZn)/A had shown Al 2p (73.67 eV), Al 2s (119.07 eV), Pt $4f_{5/2}$ (75.21 eV), Pt $4f_{7/2}$ (71.77 eV), Pt $4d_{5/2}$ (314.09 eV), Pt $4d_{5/2}$ (317.55 eV), Sn $3d_{5/2}$ (486.81 eV), Sn $3d_{3/2}$ (494.93 eV), and Zn $2p_{3/2}$ (1021.77 eV) in addition to the O 1s and Cl 2p peaks. The deconvoluted Al 2p (73.67 eV) and Al 2s (119.07 eV) peaks of Al in the case of (PtSnZn)/A catalyst showed the presence of Al^{+3}. Similarly, the deconvoluted Pt $4d_{5/2}$ (314.09 eV) and Pt $4d_{5/2}$ (317.55 eV) peaks of Pt in the case of (PtSnZn)/A catalyst indicated the presence of Pt and Pt^{+2}, respectively. The Sn was present in the form of Sn^{+4} indicated by the deconvoluted Sn $3d_{5/2}$ (486.81 eV) and Sn $3d_{3/2}$ (494.93 eV) peaks of Sn in the (PtSnZn)/A catalyst. Finally, the Zn was present in the form of Zn^{+2} as indicated in the Zn $2p_{3/2}$ (1021.77 eV) peak of Zn in the (PtSnZn)/A catalyst. Furthermore, both Pt 4f and Al2p were present together (see Figure 8(a)) in the (PtSnZn)/A catalyst like the (PtSn)/A catalyst. In summary, the active metal component of the (PtSnZn)/A catalyst was present in the form of Pt, Pt^{+2}, Al^{+3}, Sn^{+4}, and Zn^{+2} states.

These XPS results were consistent as to that of XRD analysis. Both results indicated the presence of Pt_4Sn and PtZn. Overall, the extent of the formation of Pt_4Sn in the (PtSn)/A catalyst was more as to that in the (PtSnZn)/A catalyst because of the higher Pt/Sn ration in (PtSn)A catalyst (see Table 3).

The TEM analysis of best active catalysts ((PtSn)/A and (PtSnZn)/A) is shown in Figures 9(a) and 9(b). Both the catalysts had shown a random active metal distribution up to almost similar extent. In comparison, the (PtSn)/A catalyst has better and comparatively uniform Pt particle distribution surrounded by Sn within the proximity (see Figure 9(a)). However, in the (PtSnZn)/A catalyst, the Pt particles were in the close proximity to Sn as to that of Zn (see Figures 9(a) and 9(b)).

A comparison of the (PtSn)/A and (PtSnZn)/A catalyst's stability test is shown in Figures 9(c) and 9(d) for the first cycle. Both the catalysts had shown a fairly very good stability over a cycle run of 15 hours. However, the stability of (PtSn)/A was slightly better than that of the (PtSnZn)/A catalyst. The slight variation in C2H4 selectivity in the case of (PtSnZn)/A is attributed to the presence of Zn which may had led to the formation of coking either near or in the surrounding vicinity of Pt particles.

4. Conclusions

A series of Pt/A, Sn/A, PtSn/A, SnPt/A, (PtSn)/A, (PtSn)Zn/A, and (PtSnZn)/A catalysts were prepared by using either sequential and/or simultaneous wet impregnation (see Table 1) to study the impact of catalyst preparation approach to the catalytic activity, selectivity, and yield in direct ethane dehydrogenation. Among all the studied catalysts, the (PtSn)/A and (PtSnZn)/A had shown higher initial specific activity (s^{-1}) and reaction rate constant K_d (h^{-1}) (13063.86 (s^{-1}) and 12489.69 (s^{-1}) and 0.09 (h^{-1}) and 0.06 (h^{-1})), respectively. Based on the obtained results, the catalysts prepared by using simultaneous wet impregnation had shown higher catalytic activity as to that of sequential wet impregnation. The catalyst preparation approach had direct/indirect impact to the availability and dispersion of mesoporous particles of active metal and/or promoter in the catalyst. This led to influence either to hinder the C-C cleavage and/or to promote C-H bond cleavage in the dehydrogenation of ethane to ethene. Among all studied catalysts, the (PtSn)/A had shown better catalyst stability for an experimental cycle run of 15 hours. With the increase in reaction temperature, both % conversion and % selectivity of desired reaction product were increased. The active metal component was present in the form of Pt, Pt^{+2}, Al^{+3}, Sn^{+4}, and Zn^{+2} states. The enhanced catalytic activity is attributed to the Pt_4Sn and PtZn formed phases in addition to highly dispersed mesoporous Pt particles.

Data Availability

All the data is included in the manuscript.

Conflicts of Interest

The authors declare that they have no conflicts of interest.

Acknowledgments

This project was funded by the Deanship of Scientific Research (DSR) at King Abdulaziz University, Jeddah, under grant no. G:58-135-1442. The authors, therefore, acknowledge with thanks DSR for technical and financial support.

References

[1] S. Arndt, T. Otremba, U. Simon, M. Yildiz, H. Schubert, and R. Schomäcker, "$Mn–Na_2WO_4/SiO_2$ as catalyst for the

oxidative coupling of methane. What is really known?," *Applied Catalysis A: General*, vol. 425-426, pp. 53–61, 2012.

[2] A. Cimino and F. S. Stone, "Oxide solid solutions as catalysts," in *Advances in Catalysis*, pp. 141–306, Academic Press, 2002.

[3] J. A. C. Dias and J. M. Assaf, "Influence of calcium content in Ni/CaO/γ-Al_2O_3 catalysts for CO_2-reforming of methane," *Catalysis Today*, vol. 85, no. 1, pp. 59–68, 2003.

[4] J. I. Gutiérrez-Ortiz, B. de Rivas, R. López-Fonseca, S. Martín, and J. R. González-Velasco, "Structure of Mn–Zr mixed oxides catalysts and their catalytic performance in the gas-phase oxidation of chlorocarbons," *Chemosphere*, vol. 68, no. 6, pp. 1004–1012, 2007.

[5] M. S. Lee, J. Y. Lee, D.-W. Lee, D. J. Moon, and K.-Y. Lee, "The effect of Zn addition into NiFe2O4 catalyst for high-temperature shift reaction of natural gas reformate assuming no external steam addition," *International Journal of Hydrogen Energy*, vol. 37, no. 15, pp. 11218–11226, 2012.

[6] C. Resini, M. Panizza, L. Arrighi et al., "A study of the reaction pathway upon propane oxidation over V–K/Al2O3 catalysts," *Chemical Engineering Journal*, vol. 89, no. 1–3, pp. 75–87, 2002.

[7] J. Wu, S. Mallikarjun Sharada, C. Ho, A. W. Hauser, M. Head-Gordon, and A. T. Bell, "Ethane and propane dehydrogenation over PtIr/Mg(Al)O," *Applied Catalysis A: General*, vol. 506, pp. 25–32, 2015.

[8] Y. Xu, H. Sang, K. Wang, and X. Wang, "Catalytic dehydrogenation of isobutane in the presence of hydrogen over Cs-modified Ni2P supported on active carbon," *Applied Surface Science*, vol. 316, pp. 163–170, 2014.

[9] G. Aguilar-Ríos, P. Salas, M. A. Valenzuela, H. Armendáriz, J. A. Wang, and J. Salmones, "Propane dehydrogenation activity of Pt and Pt–Sn catalysts supported on magnesium aluminate: influence of steam and hydrogen," *Catalysis Letters*, vol. 60, no. 1-2, pp. 21–25, 1999.

[10] G. Aguilar-Ríos, M. Valenzuela, P. Salas et al., "Hydrogen interactions and catalytic properties of platinum-tin supported on zinc aluminate," *Applied Catalysis A, General*, vol. 127, no. 1-2, pp. 65–75, 1995.

[11] F. M. Ashmawy, "Catalytic dehydrogenation of propane on chromia, palladium and platinum supported catalysts," *Journal of Biochemical Toxicology*, vol. 27, no. 1, pp. 137–142, 1977.

[12] A. Ates, C. Hardacre, and A. Goguet, "Oxidative dehydrogenation of propane with N2O over Fe-ZSM-5 and Fe–SiO2: influence of the iron species and acid sites," *Applied Catalysis A: General*, vol. 441-442, pp. 30–41, 2012.

[13] K. G. Azzam, G. Jacobs, W. D. Shafer, and B. H. Davis, "Dehydrogenation of propane over Pt/KL catalyst: investigating the role of L-zeolite structure on catalyst performance using isotope labeling," *Applied Catalysis A: General*, vol. 390, no. 1–2, pp. 264–270, 2010.

[14] L. Bai, Y. Zhou, Y. Zhang, H. Liu, and M. Tang, "Influence of calcium addition on catalytic properties of PtSn/ZSM-5 catalyst for propane dehydrogenation," *Catalysis Letters*, vol. 129, no. 3-4, pp. 449–456, 2009.

[15] O. A. Bariås, A. Holmen, and E. A. Blekkan, "Propane dehydrogenation over supported platinum catalysts: effect of tin as a promoter," *Catalysis Today*, vol. 24, no. 3, pp. 361–364, 1995.

[16] M. M. Bhasin, J. H. McCain, B. V. Vora, T. Imai, and P. R. Pujadó, "Dehydrogenation and oxydehydrogenation of paraffins to olefins," *Applied Catalysis A: General*, vol. 221, no. 1-2, pp. 397–419, 2001.

[17] Y.-L. Bi, K.-J. Zhen, R. X. Valenzuela, M.-J. Jia, and V. Cortés Corberán, "Oxidative dehydrogenation of isobutane over LaBaSm oxide catalyst: influence of the addition of CO2 in the feed," *Catalysis Today*, vol. 61, no. 1-4, pp. 369–375, 2000.

[18] P. Biloen, "Catalytic dehydrogenation of propane to propene over platinum and platinum-gold alloys," *Journal of Catalysis*, vol. 50, no. 1, pp. 77–86, 1977.

[19] S. A. Bocanegra, A. A. Castro, A. Guerrero-Ruíz, O. A. Scelza, and S. R. de Miguel, "Characteristics of the metallic phase of Pt/Al2O3 and Na-doped Pt/Al2O3 catalysts for light paraffins dehydrogenation," *Chemical Engineering Journal*, vol. 118, no. 3, pp. 161–166, 2006.

[20] S. A. Bocanegra, S. R. de Miguel, I. Borbath, J. L. Margitfalvi, and O. A. Scelza, "Behavior of bimetallic PtSn/Al2O3 catalysts prepared by controlled surface reactions in the selective dehydrogenation of butane," *Journal of Molecular Catalysis A: Chemical*, vol. 301, no. 1–2, pp. 52–60, 2009.

[21] F. Cavani, C. Comuzzi, G. Dolcetti et al., "Oxidative dehydrogenation of isobutane to isobutene: Dawson-type heteropolyoxoanions as stable and selective heterogeneous catalysts," *Journal of Catalysis*, vol. 160, no. 2, pp. 317–321, 1996.

[22] M. Chen, J. Xu, F. Su et al., "Dehydrogenation of propane over spinel-type gallia–alumina solid solution catalysts," *Journal of Catalysis*, vol. 256, no. 2, pp. 293–300, 2008.

[23] R. D. Cortright, J. M. Hill, and J. A. Dumesic, "Selective dehydrogenation of isobutane over supported Pt/Sn catalysts," *Catalysis Today*, vol. 55, no. 3, pp. 213–223, 2000.

[24] N. O. Elbashir, S. M. Al-Zahrani, A. E. Abasaeed, and M. Abdulwahed, "Alumina-supported chromium-based mixed-oxide catalysts in oxidative dehydrogenation of isobutane to isobutene," *Chemical Engineering and Processing: Process Intensification*, vol. 42, no. 10, pp. 817–823, 2003.

[25] M. E. Harlin, V. M. Niemi, and A. O. I. Krause, "Alumina-supported vanadium oxide in the dehydrogenation of butanes," *Journal of Catalysis*, vol. 195, no. 1, pp. 67–78, 2000.

[26] E. L. Jablonski, A. A. Castro, O. A. Scelza, and S. R. de Miguel, "Effect of Ga addition to Pt/Al2O3 on the activity, selectivity and deactivation in the propane dehydrogenation," *Applied Catalysis A: General*, vol. 183, no. 1, pp. 189–198, 1999.

[27] S. B. Kogan and M. Herskowitz, "Selective propane dehydrogenation to propylene on novel bimetallic catalysts," *Catalysis Communications*, vol. 2, no. 5, pp. 179–185, 2001.

[28] S. B. Kogan, H. Schramm, and M. Herskowitz, "Dehydrogenation of propane on modified Pt/θ-alumina performance in hydrogen and steam environment," *Applied Catalysis A: General*, vol. 208, no. 1-2, pp. 185–191, 2001.

[29] D. I. Kondarides, K. Tomishige, Y. Nagasawa, U. Lee, and Y. Iwasawa, "Characterization and performance of a [PtMo6]MgO catalyst for alkane-to-alkene conversion," *Journal of Molecular Catalysis A: Chemical*, vol. 111, no. 1-2, pp. 145–165, 1996.

[30] M.-H. Lee, B. M. Nagaraja, P. Natarajan et al., "Effect of potassium addition on bimetallic PtSn/θ-Al2O3 catalyst for dehydrogenation of propane to propylene," *Research on Chemical Intermediates*, vol. 42, no. 1, pp. 123–140, 2016.

[31] Q. Li, Z. Sui, X. Zhou, and D. Chen, "Kinetics of propane dehydrogenation over Pt–Sn/Al2O3 catalyst," *Applied Catalysis A: General*, vol. 398, no. 1-2, pp. 18–26, 2011.

[32] Y. Li, Z. Zhang, J. Wang, C. Ma, H. Yang, and Z. Hao, "Direct dehydrogenation of isobutane to isobutene over carbon

catalysts," *Chinese Journal of Catalysis*, vol. 36, no. 8, pp. 1214–1222, 2015.

[33] J. Llorca, N. Homs, J. León, J. Sales, J. L. G. Fierro, and P. Ramirez de la Piscina, "Supported Pt–Sn catalysts highly selective for isobutane dehydrogenation: preparation, characterization and catalytic behavior," *Applied Catalysis A: General*, vol. 189, no. 1, pp. 77–86, 1999.

[34] M. P. Lobera, C. Téllez, J. Herguido, and M. Menéndez, "Transient kinetic modelling of propane dehydrogenation over a Pt–Sn–K/Al2O3 catalyst," *Applied Catalysis A: General*, vol. 349, no. 1-2, pp. 156–164, 2008.

[35] S. Luo, N. Wu, B. Zhou, S.-b. He, J.-s. Qiu, and C.-l. Sun, "Effect of alumina support on the performance of Pt- Sn-K/γ-Al_2O_3 catalyst in the dehydrogenation of isobutane," *Journal of Fuel Chemistry and Technology*, vol. 41, no. 12, pp. 1481–1487, 2013.

[36] Z. Ma, Y. Mo, J. Li, C. An, and X. Liu, "Optimization of PtSnK/Al2O3 isobutane dehydrogenation catalyst prepared by an impregnation-reduction method," *Journal of Natural Gas Science and Engineering*, vol. 27, Part 2, pp. 1035–1042, 2015.

[37] M. Ohta, Y. Ikeda, and A. Igarashi, "Preparation and characterization of Pt/ZnO-Cr_2O_3 catalyst for low-temperature dehydrogenation of isobutane," *Applied Catalysis A: General*, vol. 258, no. 2, pp. 153–158, 2004.

[38] M. Ohta, Y. Ikeda, and A. Igarashi, "Additive effect of Sn in Pt–Sn/ZnO–Cr_2O_3 catalyst for low-temperature dehydrogenation of isobutane," *Applied Catalysis A: General*, vol. 266, no. 2, pp. 229–233, 2004.

[39] G. J. Siri, G. R. Bertolini, M. L. Casella, and O. A. Ferretti, "PtSn/γ-Al2O3 isobutane dehydrogenation catalysts: the effect of alkaline metals addition," *Materials Letters*, vol. 59, no. 18, pp. 2319–2324, 2005.

[40] G. J. Siri, M. L. Casella, G. F. Santori, and O. A. Ferretti, "Tin/platinum on alumina as catalyst for dehydrogenation of isobutane. Influence of the preparation procedure and of the addition of lithium on the catalytic properties," *Industrial & Engineering Chemistry Research*, vol. 36, no. 11, pp. 4821–4826, 1997.

[41] Y. Takita, X. Qing, A. Takami, H. Nishiguchi, and K. Nagaoka, "Oxidative dehydrogenation of isobutane to isobutene III: reaction mechanism over CePO4 catalyst," *Applied Catalysis A: General*, vol. 296, no. 1, pp. 63–69, 2005.

[42] Y.-P. Tian, P. Bai, S.-M. Liu, X.-M. Liu, and Z.-F. Yan, "VOx–K2O/γ-Al2O3 catalyst for nonoxidative dehydrogenation of isobutane," *Fuel Processing Technology*, vol. 151, pp. 31–39, 2016.

[43] N. V. Vernikovskaya, I. G. Savin, V. N. Kashkin et al., "Dehydrogenation of propane–isobutane mixture in a fluidized bed reactor over Cr2O3/Al2O3 catalyst: experimental studies and mathematical modelling," *Chemical Engineering Journal*, vol. 176-177, pp. 158–164, 2011.

[44] V. P. Vislovskiy, N. T. Shamilov, A. M. Sardarly et al., "Oxidative conversion of isobutane to isobutene over V-Sb-Ni oxide catalysts," *Applied Catalysis A: General*, vol. 250, no. 1, pp. 143–150, 2003.

[45] B. V. Vora, "Development of dehydrogenation catalysts and processes," *Topics in Catalysis*, vol. 55, no. 19-20, pp. 1297–1308, 2012.

[46] H. F. Abbas and W. M. A. Wan Daud, "Hydrogen production by methane decomposition: a review," *International Journal of Hydrogen Energy*, vol. 35, no. 3, pp. 1160–1190, 2010.

[47] V. Iannazzo, G. Neri, S. Galvagno, M. Di Serio, R. Tesser, and E. Santacesaria, "Oxidative dehydrogenation of isobutane over V_2O_5-based catalysts prepared by grafting vanadyl alkoxides on TiO_2·SiO_2 supports," *Applied Catalysis A: General*, vol. 246, no. 1, pp. 49–68, 2003.

[48] G. A. Martin and C. Mirodatos, "Surface chemistry in the oxidative coupling of methane," *Fuel Processing Technology*, vol. 42, no. 2–3, pp. 179–215, 1995.

[49] P. Moriceau, B. Grzybowska, Y. Barbaux, G. Wrobel, and G. Hecquet, "Oxidative dehydrogenation of isobutane on Cr–Ce–O oxide:: I. Effect of the preparation method and of the Cr content," *Applied Catalysis A: General*, vol. 168, no. 2, pp. 269–277, 1998.

[50] F. Sala and F. Trifiró, "Relationship between structure and activity of antimony mixed oxides in 1-butene oxidation," *Journal of Catalysis*, vol. 41, no. 1, pp. 1–13, 1976.

[51] J. C. Serrano-Ruiz, A. Sepulveda-Escribano, and F. Rodriguez-Reinoso, "Bimetallic PtSn/C catalysts promoted by ceria: application in the nonoxidative dehydrogenation of isobutane," *Journal of Catalysis*, vol. 246, no. 1, pp. 158–165, 2007.

[52] H. Shimada, T. Akazawa, N.-O. Ikenaga, and T. Suzuki, "Dehydrogenation of isobutane to isobutene with iron-loaded activated carbon catalyst," *Applied Catalysis A: General*, vol. 168, no. 2, pp. 243–250, 1998.

[53] T. Otroshchenko, J. Radnik, M. Schneider, U. Rodemerck, D. Linke, and E. V. Kondratenko, "Bulk binary ZrO2-based oxides as highly active alternative-type catalysts for non-oxidative isobutane dehydrogenation," *Chemical Communications*, vol. 52, no. 52, pp. 8164–8167, 2016.

[54] U. Rodemerck, E. V. Kondratenko, T. Otroshchenko, and D. Linke, "Unexpectedly high activity of bare alumina for non-oxidative isobutane dehydrogenation," *Chemical Communications*, vol. 52, no. 82, pp. 12222–12225, 2016.

[55] U. Rodemerck, S. Sokolov, M. Stoyanova, U. Bentrup, D. Linke, and E. V. Kondratenko, "Influence of support and kind of VOx species on isobutene selectivity and coke deposition in non-oxidative dehydrogenation of isobutane," *Journal of Catalysis*, vol. 338, pp. 174–183, 2016.

[56] J. Nam and F. E. Celik, "Effect of tin in the bulk of platinum–tin alloys for ethane dehydrogenation," *Topics in Catalysis*, vol. 63, no. 7-8, pp. 700–713, 2020.

[57] Q. Zhang, K. Zhang, S. Zhang et al., "Ga3+-stabilized Pt in PtSn-Mg(Ga)(Al)O catalyst for promoting ethane dehydrogenation," *Journal of Catalysis*, vol. 368, pp. 79–88, 2018.

[58] A. M. Ali, A. A. Zahrani, M. A. Daous, M. U. S. Podila, and L. A. Petrov, "Highly active and selective PtSnM1/gamma-Al2O3 catalyst for direct propane dehydrogenation," *Journal of the Chemical Society of Pakistan*, vol. 43, no. 3, pp. 342–360, 2021.

[59] F. M. Li, H. Q. Yang, T. Y. Ju, X. Y. Li, and C. W. Hu, "Activation of propane C-H and C-C bonds by gas-phase Pt atom: a theoretical study," *International Journal of Molecular Sciences*, vol. 13, no. 7, pp. 9278–9297, 2012.

[60] S.-U. Lee, Y.-J. Lee, S.-J. Kwon, J.-R. Kim, and S.-Y. Jeong, "Pt-Sn supported on beta zeolite with enhanced activity and stability for propane dehydrogenation," *Catalysts*, vol. 11, no. 1, p. 25, 2021.

[61] P. D. Zgolicz, V. I. Rodríguez, I. M. J. Vilella, S. R. de Miguel, and O. A. Scelza, "Catalytic performance in selective hydrogenation of citral of bimetallic Pt–Sn catalysts supported on

MgAl2O4 and γ-Al2O3," *Applied Catalysis A: General*, vol. 392, no. 1-2, pp. 208–217, 2011.

[62] F. Lin, R. Delmelle, T. Vinodkumar, B. M. Reddy, A. Wokaun, and I. Alxneit, "Correlation between the structural characteristics, oxygen storage capacities and catalytic activities of dual-phase Zn-modified ceria nanocrystals," *Catalysis Science & Technology*, vol. 5, no. 7, pp. 3556–3567, 2015.

[63] D. Guillaume, S. Gautier, I. Despujol, F. Alario, and P. Beccat, "Characterization of acid sites on γ-alumina and chlorinated γ-alumina by 31P NMR of adsorbed trimethylphosphine," *Catalysis Letters*, vol. 43, no. 3-4, pp. 213–218, 1997.

[64] W. Kania and K. Jurczyk, "Acid-base properties of modified γ-alumina," *Applied Catalysis*, vol. 34, pp. 1–12, 1987.

[65] S. Bing-Jian, K.-W. Wang, C.-J. Tseng, C.-H. Wang, and Y.-J. Hsueh, "Synthesis and catalytic property of PtSn/C toward the ethanol oxidation reaction," *International Journal of Electrochemical Science*, vol. 7, no. 6, pp. 5246–5255, 2012.

[66] A. Bonesi, W. E. Triaca, and A. M. C. Luna, "Nanocatalysts for ethanol oxidation. Synthesis and characterisation," *Portugaliae Electrochimica Acta*, vol. 27, no. 3, pp. 193–201, 2009.